MOLECULAR AND CELLULAR BIOLOGY, Mar. 2008, p. 1936–1946 Vol. 28, No. 6
0270-7306/08/$08.00+0 doi:10.1128/MCB.01701-07


# Loss of Singleminded-2s in the Mouse Mammary Gland Induces an Epithelial-Mesenchymal Transition Associated with Up-Regulation of Slug and Matrix Metalloprotease 2▽†

Brian Laffin,[1] Elizabeth Wellberg,[1] Hyeong-Il Kwak,[1] Robert C. Burghardt,[1] Richard P. Metz,[1] Tanya Gustafson,[1] Pepper Schedin,[2] and Weston W. Porter[1]*

*Department of Integrated Biosciences, College of Veterinary Medicine, Texas A&M University, College Station, Texas 77843,[1] and AMC Cancer Research Center and Department of Medicine, University of Colorado Cancer Center, University of Colorado Health Sciences Center, Aurora, Colorado 80045[2]*

Received 14 September 2007/Returned for modification 14 October 2007/Accepted 13 December 2007

**The short splice variant of the basic helix-loop-helix Per-Arnt-Sim transcription factor Singleminded-2, SIM2s, has been implicated in development and is frequently lost or reduced in primary breast tumors. Here, we show that loss of Sim2s causes aberrant mouse mammary gland ductal development with features suggestive of malignant transformation, including increased proliferation, loss of polarity, down-regulation of E-cadherin, and invasion of the surrounding stroma. Additionally, knockdown of SIM2s in MCF-7 breast cancer cells contributed to an epithelial-mesenchymal transition (EMT) and increased tumorigenesis. In both Sim2$^{-/-}$ mammary glands and SIM2s-depleted MCF7 cells, these changes were associated with increased SLUG and MMP2 levels. SIM2s protein was detectable on the SLUG promoter, and overexpression of SIM2s repressed expression from a SLUG-controlled reporter in a dose-dependent manner. To our knowledge, SIM2s is the first protein shown to bind and repress the SLUG promoter, providing a plausible explanation for the development role and breast tumor-suppressive activity of SIM2s. Together, our results suggest that SIM2s is a key regulator of mammary-ductal development and that loss of SIM2s expression is associated with an invasive, EMT-like phenotype.**

Branching morphogenesis is a tightly regulated, complex process that contributes to lung, kidney, central nervous system (CNS), and mammary gland development. In the developing mammary gland, cell division and migration are confined to the cap cell layer at the leading edges of terminal end buds (TEBs), which invade the surrounding fat pad, leaving behind the basic mammary-ductal tree (37, 38). Cells trailing TEBs stop dividing, form a hollow tube through an apoptotic mechanism, and differentiate into polarized luminal epithelial cells. Proper regulation of mammary epithelium- and stroma-derived signals is paramount to ensuring correct temporal and spatial control of these processes, and disruption of epithelial-stromal communication is associated with breast cancer initiation and progression. While branching morphogenesis differs between tissues, there are a large number of shared molecular mechanisms, suggesting that a "branching module" of signaling pathways exists (5).

In the developing *Drosophila* CNS, specification of the CNS midline is dependent upon the basic helix-loop-helix Per-Arnt-Sim transcription factor single-minded (sim), which serves as the master regulator of midline differentiation. Singleminded-2 (SIM2) is one of two vertebrate orthologs of *Drosophila sim* protein, but it differs in functioning as a transcriptional repressor (10, 24, 30). SIM2 was initially identified by positional cloning around the Down syndrome critical region of chromosome 21 and is believed to contribute to many of the physiological abnormalities associated with trisomy 21 (4). Sim2 plays an important role in development, as Sim2 null mice die shortly after birth due to multiple abnormalities, including cleft palate, improper diaphragm development, and rib defects (12, 33). The molecular mechanisms controlling these processes are complex and involve the concerted actions of many factors, including transforming growth factor β, epidermal growth factor receptor, and matrix metalloproteases (MMPs) (3, 23, 36). These pathways are also known to contribute to pathological conditions, including tumor progression and metastasis. The fact that Sim2$^{-/-}$ mice have these defects suggests that Sim2 regulates pathways involved in growth and motility.

During morphogenesis, epithelial-to-mesenchymal transitions (EMTs) play an important role in regulating cellular migration and establishment of new tissue types (34). Similar transitions commonly occur during cancer progression and metastasis, leading to increased tumor cell motility and invasion. Loss of the cell-cell adhesion molecule E-cadherin is central to EMT, and invasive lobular carcinomas of the breast often exhibit loss of E-cadherin expression or function (17, 21). Similar to fate determination in the *Drosophila* midline, induction of EMT by the transcription factors SNAIL, SLUG, and TWIST is dependent upon their abilities to silence expression from the E-cadherin promoter; however, the molecular mechanisms acting upstream of these factors are not well characterized (17, 21).

Previously, we showed that human breast luminal epithelial cells primarily express the short splice variant of SIM2, SIM2s,

* Corresponding author. Mailing address: Department of Integrated Biosciences, College of Veterinary Medicine, Texas A&M University, College Station, TX 77843. Phone: (979) 845-0733. Fax: (979) 862-4929. E-mail: wporter@cvm.tamu.edu.

† Supplemental material for this article may be found at http://mcb.asm.org/.

▽ Published ahead of print on 26 December 2007.

which acts as a breast tumor suppressor (20). In the present study, we report that loss of Sim2s in mouse mammary epithelium leads to increased proliferation, loss of E-cadherin, and invasion into the surrounding stroma. Furthermore, vector-based short hairpin RNA (shRNA) silencing of SIM2s in the human breast cancer cell line MCF-7 promoted EMT and increased tumorigenesis. Concomitant with this phenotype, loss of SIM2s resulted in dysregulation of MMP2 and SLUG expression. These results suggest that SIM2s plays a key role in controlling normal EMT processes involved in mammary gland development and that loss of SIM2s promotes pathological EMT events associated with tumor progression.

## MATERIALS AND METHODS

**Cell culture.** The cell lines used in these studies were obtained from the American Type Culture Collection and were maintained as recommended. HEK-293T Ampho-Phoenix packaging cells were obtained with permission from Gary Nolan at Stanford University.

**Animals.** Female C57BL/6J and nude mice were from Jackson Laboratories. The Sim2 knockout mice were obtained from a private collection at Jackson Laboratories with permission from Michael Shamblott at Johns Hopkins University. All animals were housed three per cage under a standard 12-hour photoperiod. The animals were provided with access to food and water ad libitum. All procedures were approved by the University Laboratory Animal Care Committee at Texas A&M University.

**Generation of stable shRNA-expressing cell lines.** pSilencer U6 retro 5.1 expression vectors (Ambion, Austin, TX) bearing either one of three SIM2-specific or a nonspecific scrambled control (SCR) insert were packaged into virus using Phenix HEK293-Ampho packaging cells and used to transduce MCF-7 cells according to the manufacturer's protocol. Pooled populations of the two most effective of the three SIM2-specific constructs, SIM2$i_{3116}$ (SIM2*i*) and SIM2$i_{114478}$ (SIM2$i_2$), were confirmed to decrease SIM2 protein levels, and SIM2*i* was used for all subsequent studies. A third SIM2-targeting sequence, SIM2$i_{114477}$ (SIM2$i_3$), was also analyzed but failed to decrease SIM2 expression. Cells were selected in the presence of 2 μg/ml puromycin based on kill curves of mock-infected MCF-7 cells. The MCF-7 shRNA cell lines analyzed were pooled populations, not selected single-cell clones.

**Invasion assays.** Invasion was measured using control and Matrigel-coated invasion chambers (Falcon BD, Franklin Lakes, NJ). A total of 12,500 cells were seeded in serum-free Dulbecco's modified Eagle's medium (DMEM) in the upper chamber, with serum-containing medium in the lower chamber as a chemoattractant. After 20 h at 37°C, cells were scraped from the upper chamber with a cotton swab, and the undersides of the membranes were fixed in 100% MeOH, stained with DAPI (4′,6′-diamidino-2-phenylindole), and counted. The percent invasion was calculated according to the manufacturer's instructions.

**Real-time RT-PCR.** RNA isolation and real-time reverse transcription (RT)-PCR were performed as described previously (20). Primer sequences are listed in Table S1 in the supplemental material. Product specificity was examined by dissociation curve analysis.

**Immunoblotting and zymography.** Cells were lysed on ice in RIPA buffer (phosphate-buffered saline [PBS] containing 1% Igepal CA630, 0.5% sodium deoxycholate, and 0.1% sodium dodecyl sulfate) containing protease inhibitors and 20 μM MG132. The lysates were cleared by centrifugation, and 50 μg of total protein was separated on sodium dodecyl sulfate-polyacrylamide gel electrophoresis gels and transferred to polyvinylidene difluoride membranes. Primary antibodies and conditions are listed in Table S2 in the supplemental material. All secondary antibodies were used at a 1:5,000 dilution. Immunoblots were visualized with an ECL kit (Amersham). To determine MMP activity, conditioned medium from treated cells was concentrated ~20-fold using Centricon 10 spin concentrators (Amicon). Equal amounts of protein were mixed with Laemmli sample buffer without reducing agents, incubated for 15 min at 37°C, and separated on 8% polyacrylamide slab gels containing 1 mg/ml gelatin or 0.05% casein. Following electrophoresis, the gels were placed in 2.5% Triton X-100 for 30 min and then incubated at 37°C in 50 mM Tris-HCl, pH 7.4, containing 5 mM $CaCl_2$ for 18 h. MMP activity was visualized by Coomassie blue staining.

**Immunofluorescence analysis and phase-contrast microscopy.** Primary antibodies and conditions for immunostaining are listed in Table S2 in the supplemental material. Monolayers grown on glass coverslips were prepared for immunofluorescence analysis by washing them twice in PBS, followed by fixation with 3.8% paraformaldehyde, permeabilization in 0.5% Triton X-100, and two rinses in 100 mM glycine. Blocking was performed for 2 h in PBS containing 5% bovine serum albumin, and primary antibodies were applied overnight in blocking solution. Mammary gland and xenograft tumor sections on Superfrost plus microscope slides were baked at 60°C for 30 min in an upright position and then rehydrated by sequential washes in xylene and a series of graded ethanol washes. Antigen retrieval was performed for 15 min at 98°C in 0.01 mol/liter sodium citrate buffer, pH 6.0, in a microwave oven. When appropriate, sections were incubated in 3% hydrogen peroxide for 6 min to block endogenous peroxidase activity. After a 45-min block in 10% serum, the sections were incubated with the primary antibody for 2 h at room temperature or overnight at 4°C. Secondary detection was performed with a fluorescent secondary antibody or the appropriate biotinylated secondary antibody, a Vectastain ABC elite kit, and 3,3′-diaminobenzidine (Vector Laboratories, Burlingame, CA). DAPI, fluorescent Alexa Fluor-conjugated secondary antibodies, and phalloidin were purchased from Molecular Probes and applied according to the manufacturer's instructions. For phase-contrast analysis, cells were grown on glass coverslips and visualized in 10% DMEM. All microscopic images were taken with a Zeiss Axioplan 2 microscope (Carl Zeiss, Thornwood, NY) fitted with an Axiocam high-resolution digital camera and using Axiovision 4.1 software.

**Nude-mouse xenograft tumor studies.** Either Scr or SIM2*i* MCF-7 cells ($1 \times 10^7$) suspended in 100 μl of DMEM-50% Matrigel (BD Biosciences) were injected into each flank of nude mice. Tumor size was measured with calipers on days 3, 10, 14, and 17. The mice were injected with bromodeoxyuridine (BrdU) (Amersham) 2 h prior to sacrifice on day 17. Tumors and tissues were removed, photographed, weighed, and frozen for subsequent RNA and protein extraction. Half of the tissue was fixed in 4% paraformaldehyde, embedded in paraffin, and sectioned.

**Chromatin immunoprecipitation (ChIP) assays and transient transfections.** Transient-transfection experiments and ChIP assays were performed as described previously (22). Primer sequences are presented in Table S1 in the supplemental material.

**Mammary gland transplantation and whole-mount analysis.** Mammary tissue from day 1 pups was dissected out and transferred into the cleared number 4 mammary fat of nude mice. After 8 weeks, the transplants were removed, fixed in 10% neutral-buffered formalin, and analyzed by whole-mount analysis. Hematoxylin and eosin (HE) and trichrome staining of sections was performed by the Department of Integrated Biosciences Histology Core Facility at Texas A&M University.

**Statistical analyses.** Statistical analyses for these studies were performed using Student's *t* test. The errors bars in graphs represent standard errors of the mean (SEM) in all cases.

## RESULTS

**Sim2s expression is spatially and temporally regulated in the developing mouse mammary gland.** Mammary gland development is regulated through a branching-morphogenesis mechanism driven by the growth of TEBs, which are characterized by a highly proliferative and invasive "cap cell" layer that divides and invades the surrounding stroma. TEBs are controlled by a complex balance of stroma- and epithelium-derived signals that guide TEB growth, ensuring orderly development of a mammary-ductal structure. The developmental defects observed in Sim2$^{-/-}$ mice, coupled with its antitumorigenic effects in breast cancer-derived cell lines (20), suggest a possible developmental role for Sim2 in the mammary gland. Indeed, Western blot analysis found that, similar to the human breast (20), Sim2s is the predominant Sim2 isoform expressed in 15-week-old virgin-mouse mammary glands (Fig. 1A), whereas skeletal muscle expressed both the short and long isoforms (22). In addition, Sim2s was detectible in ductal epithelial cells (Fig. 1B), supporting a role for Sim2s in mammary gland development.

**Aberrant ductal development and hyperplasia in Sim2$^{-/-}$ mouse mammary glands.** Since Sim2$^{-/-}$ mice die shortly after birth (12, 33), wild-type (WT) and Sim2$^{-/-}$ mammary buds from

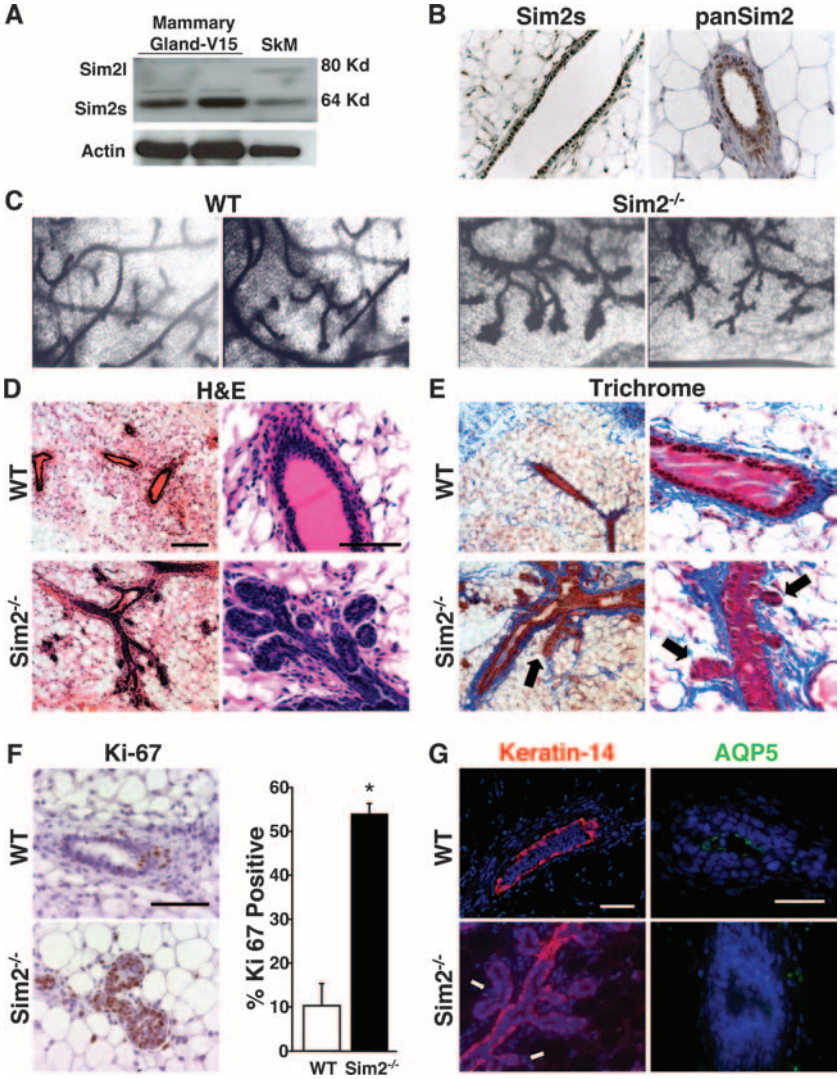


FIG. 1. Sim2 is required for normal mammary-ductal development in mice. Mammary buds were removed from 1-day-old WT and Sim2$^{-/-}$ neonates and transplanted contralaterally into the cleared inguinal mammary fat pads of nude mice. Following 8 weeks of outgrowth, the mammary glands were removed and fixed for whole-mount staining and sectioning. (A) Western blot analysis of mammary glands from 15-week-old virgin mice and skeletal muscle using a pan-Sim2-specific antibody showing that Sim2s is expressed in the developing mouse mammary gland, whereas skeletal muscles express both isoforms. β-Act, actin. (B) Immunohistochemical analyses using antibodies specific to the Sim2s isoform and a pan-Sim2-specific antibody showing Sim2s expression in luminal epithelial cells. (C) Representative images of hematoxylin-stained whole mounts of WT and Sim2$^{-/-}$ mammary outgrowths showing bud-like structures on Sim2$^{-/-}$ mammary ducts. (D) HE-stained sections from WT (top) and Sim2$^{-/-}$ (bottom) mammary outgrowths showing filled ducts (bottom left) and a detailed image of budding structures (bottom right) in Sim2$^{-/-}$ mammary glands. (E) Representative images of Masson's trichrome-stained mammary sections from WT (top) and Sim2$^{-/-}$ (bottom) mammary glands. The arrows indicate areas of collagen depletion and apparent Sim2$^{-/-}$ epithelial cell invasion into the surrounding stroma. (F) Ki-67-stained sections of WT (top) and Sim2$^{-/-}$ (bottom) mammary glands indicating that Sim2 loss significantly increases cellular proliferation. Quantification of Ki-67-positive cells (right) suggested that Sim2$^{-/-}$ glands experience a greater-than-fivefold increase in cell division. The data are represented as the mean plus SEM; * indicates that $P$ was $<0.05$. (G) Immunofluorescence staining for keratin 14 (red; left colum) and aquaporin 5 (green; right column) in WT (top row) and Sim2$^{-/-}$ (bottom row) mammary glands. Note that the "budding" Sim2$^{-/-}$ epithelial cells are not surrounded by a keratin 14-positive myoepithelial cell layer (arrows), suggesting they are actively invading the surrounding stroma. Aquaporin 5 staining (right) highlights the compromised polarity observed in Sim2$^{-/-}$ mammary epithelium. Bars = 100 μm.

day 1 neonates were rescued and transplanted contralaterally into cleared inguinal mammary fat pads of nude mice. After 8 weeks, WT and Sim2$^{-/-}$ outgrowths were removed and analyzed. Gross observation of whole-mount stained mammary outgrowths highlighted subtle differences in the morphology of Sim2$^{-/-}$ ducts. Most notably, Sim2$^{-/-}$ ducts appeared to have increased alveolar budding reminiscent of an increase in differentiation (Fig. 1C). However, HE-stained sections of WT and Sim2$^{-/-}$ mammary outgrowths revealed that Sim2$^{-/-}$ ducts had failed to hollow and that the bud-like structures were comprised of disorganized epithelial cells (Fig. 1D). Furthermore, Masson's trichrome staining revealed that the basement and interstitial membranes surrounding Sim2$^{-/-}$ glands appeared to be disrupted, with noticeable regions of collagen depletion (Fig. 1E, left). Upon closer exami-

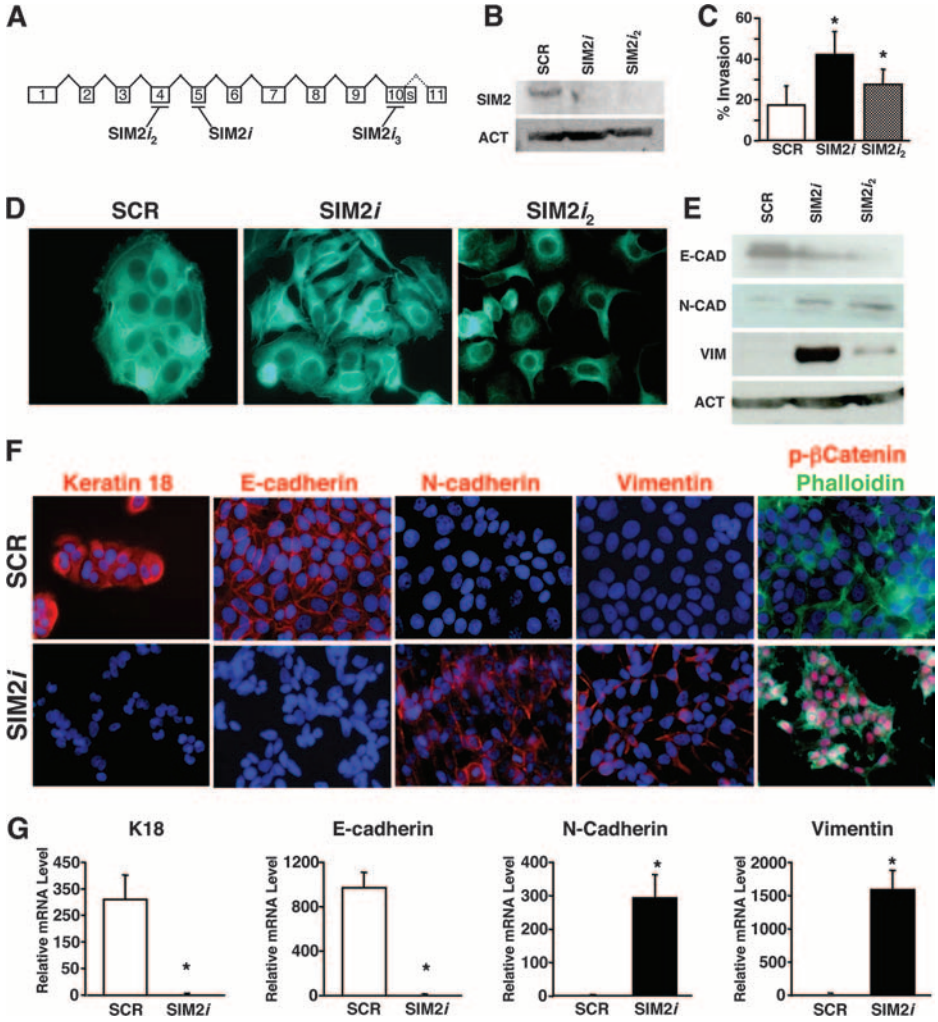


FIG. 2. Silencing of SIM2s alters cellular morphology, increases invasive potential, and causes EMT in MCF-7 cells. (A) Structure of the SIM2s mRNA transcript showing regions targeted by shRNA constructs. Exons are indicated by numbered boxes. The dotted line indicates splicing that generates the full-length SIM2 transcript. (B) Infection of MCF-7 cells with shRNA construct SIM2*i* or SIM2$i_2$ resulted in decreased SIM2s protein levels in comparison to a nonspecific SCR shRNA construct. Down-regulation of SIM2s expression by the SIM2$i_3$ construct could not be confirmed (data not shown). (C) Down-regulation of SIM2s significantly increased MCF-7 cell invasive ability. The data are represented as the mean plus SEM; ∗ indicates that $P$ was $<0.05$. (D) Phaloidin-stained control (SCR) and SIM2*i* MCF-7 cells indicated that decreased SIM2s expression correlated with alterations in cellular morphology. SIM2*i* cells showed a loss of the cobblestone morphology seen in SCR MCF-7 cells and acquisition of a more spindly appearance. (E) Decreased SIM2s expression leads to loss of E-cadherin and gain of vimentin. (F) Immunofluorescent staining of control (SCR) (top) and SIM2*i* (bottom) MCF-7 cells showing that loss of SIM2s expression results in loss of the epithelial markers E-cadherin and keratin 18 and gain of the mesenchymal markers N-cadherin and vimentin and thus a switch from an epithelial to a more mesenchymal phenotype. In addition, increased nuclear staining of phosphorylated β-catenin, a phenomenon recently associated with poor breast cancer prognosis, can be seen in SIM2*i* cells. (G) Western blot and real-time quantitative PCR analyses of SCR and SIM2*i* MCF-7 cells for expression of keratin 18 (K18), E-cadherin, N-cadherin, and vimentin mRNAs. The data were obtained from three wells per group and analyzed by the $\Delta\Delta CT$ method and are expressed as the average difference plus SEM; ∗, $P > 0.05$. Combined with the altered cell morphology and gain of invasive potential, these data suggest that loss of SIM2s expression in MCF-7 cells induces an EMT.

nation, $Sim2^{-/-}$ epithelial cells could be seen breaking through these membranes and migrating into the surrounding stroma (Fig. 1E, right). The filled ducts observed in $Sim2^{-/-}$ glands were likely due to increased proliferation, as $Sim2^{-/-}$ mammary epithelial cells displayed a fivefold increase in staining for the proliferation marker Ki-67 (Fig. 1F), and terminal deoxynucleotidyltransferase-mediated dUTP-biotin nick end labeling analyses did not show significant differences in apoptosis (data not shown). Keratin 14 staining indicated that the myoepithelial cell layer of $Sim2^{-/-}$ ducts was intact, while $Sim2^{-/-}$ epithelial cells appeared to have invaded the surrounding stroma (Fig. 1G, left). This phenomenon is distinct from normal side branching and is consistent with a more aggressive phenotype. Staining for aquaporin 5, an apical epithelial cell marker, suggested that the lumens occasionally seen in larger $Sim2^{-/-}$ ducts were lined primarily with nonpolarized cells, implying that Sim2 loss has a significant impact on mammary epithelial organization (Fig. 1H, right).

**Silencing SIM2s induces EMT in MCF-7 cells.** Previously, we showed that SIM2s expression is lost in human breast tumors and correlates inversely with breast cancer cell invasive-

ness (20). Reintroduction of SIM2s into highly invasive cancer cells resulted in decreased proliferation, migration, and invasion. To further delineate the role of SIM2s in cancer progression, MCF-7 cells were transduced with either a nonspecific SCR shRNA retroviral construct or one of three SIM2-specific shRNA constructs targeting different regions of the SIM2 mRNA (SIM2$i_2$, SIM2*i*, and SIM2$i_3$) (Fig. 2A). Significant reduction in SIM2s protein was observed in the SIM2$i_2$ and SIM2*i* cell lines (Fig. 2B), but not in SIM2$i_3$ cells (data not shown). In three independent infections, pooled populations of MCF-7 SIM2*i* and SIM2$i_2$ cells showed significantly enhanced invasive abilities (Fig. 2C) and underwent a morphological change from the cobblestone epithelial shape typical of MCF-7 cells to a spindly mesenchymal-cell-like morphology (Fig. 2D), suggesting that loss of SIM2s expression had induced EMT. Indeed, Western blots (Fig. 2E) confirmed that SIM2*i* and SIM2$i_2$ cells lost E-cadherin and increased expression of N-cadherin and vimentin.

To confirm that the morphological and biochemical changes observed with the loss of SIM2s were indeed an EMT, we characterized further the SIM2*i* MCF-7 cell line to assay for expression of additional epithelial and mesenchymal cell markers. Immunofluorescence (Fig. 2F) showed that SIM2*i* cells lost expression of keratin 18 and E-cadherin and gained N-cadherin and vimentin. Although SIM2*i* MCF-7 cells express mesenchymal markers and do not express E-cadherin, increased nuclear accumulation of β-catenin was not detectable by antibodies against the active, nonphosphorylated (S37 and T41) form (data not shown). There was, however, a marked increase in nuclear accumulation of the phospho-S33, -S37, and -T41 forms of β-catenin (Fig. 2F), a phenomenon recently shown to be associated with poor prognosis in aggressive breast carcinomas (26). Changes in SIM2s protein levels were accompanied by dramatic decreases in keratin 18 and E-cadherin message and increased N-cadherin and vimentin mRNAs, as measured by real-time RT-PCR (Fig. 2G). Together, these data indicate that loss of SIM2s in MCF-7 cells results in a morphological, functional, and biochemical switch from an epithelial to a more mesenchymal-like phenotype.

**SIM2*i* MCF-7 cells form rapidly growing estrogen receptor α$^-$ (ERα$^-$) tumors in nude mice.** To assess the tumorigenic effects of SIM2s loss, we compared the tumor-forming ability of SIM2*i* cells to that of control cells using a nude-mouse xenograft assay. SIM2*i* cells rapidly developed into tumors that were three times larger than controls by day 10 (Fig. 3A). SIM2*i* cell-derived tumors maintained this size advantage throughout the experiment and were sixfold larger than SCR-derived tumors, with an average weight sevenfold higher than that of control tumors at the conclusion of the study 17 days after injection (Fig. 3B). SIM2*i* tumors appeared to be more vascularized than control tumors (Fig. 3C), an observation that was confirmed by increased CD31 and vascular endothelial growth factor immunoreactivity (Fig. 3D). Quantification of BrdU-positive cells from xenograft tumor sections showed a 35-fold increase in SIM2*i* cell proliferation (Fig. 3E) (SCR = 1.1% ± 0.543%; SIM2*i* = 35.1% ± 2.24%), suggesting a link between increased vascularity, cell proliferation, and tumor growth in SIM2*i*-derived tumors. This sizable increase in proliferation was unexpected, as the SIM2*i* cells do not proliferate more rapidly than the SCR control MCF-7 cell line in vitro (data not shown). Similar to our in vitro studies (Fig. 2), SIM2*i*-derived tumors displayed signs of EMT with decreased E-cadherin and increased vimentin staining (Fig. 3D).

Normally, tumor development in the MCF-7 xenograft model requires exogenous estrogen to sustain growth. Therefore, we were surprised to see tumors develop so rapidly in the absence of estrogen. The accelerated rate of SIM2*i* tumor growth coupled with the apparent estrogen-independent nature of this growth prompted us to look at ERα expression. Indeed, ERα was undetectable in SIM2*i*-derived tumors by immunohistochemistry (Fig. 3D) or in SIM2*i* MCF-7 cells by either real-time RT-PCR (Fig. 4A) or Western blotting (Fig. 4B). Furthermore, SIM2*i* cells no longer responded to estrogen treatment as measured by estrogen-induced proliferation (data not shown) and induction of the estrogen-responsive genes PR and PS2 (Fig. 4C and D). The striking increase in SIM2*i* MCF-7 cell tumorigenesis confirms that loss of SIM2 has functional consequences in vivo and provides further evidence that SIM2s may represent an important hurdle to breast cancer progression.

**SIM2s represses MMP2 expression and activity.** In previous studies utilizing MDA-MB-435 cells, we reported that MMP3 is a direct target of SIM2s-mediated transcriptional repression (20). Therefore, we hypothesized that up-regulation of MMPs may contribute to the aggressive, invasive phenotype observed in SIM2s-compromised cells. Expression of several MMPs, and related factors, was analyzed in SCR and SIM2*i* cells by real-time PCR. To our surprise, we found MMP2 to be up-regulated >4,500-fold in SIM2*i* cells, while MMP3 mRNA expression was not significantly altered (Fig. 5A). MMP14 and TIMP2, which are required for MMP2 activation, were also up-regulated approximately six- and sevenfold, respectively, in SIM2*i* cells (Fig. 5A). The MMP2 mRNA increase observed in SIM2*i* cells was corroborated at the protein and activity levels, while MMP3 protein expression and activity were unchanged (Fig. 5B). In addition, MMP2 levels were markedly elevated in xenograft tumor sections derived from SIM2*i* cells in comparison to those derived from control cells (Fig. 5C), confirming that loss of SIM2s led to increased MMP2 expression. Increased MMP2 expression was attributable to derepression of the MMP2 promoter, as expression of an MMP2-controlled luciferase reporter was significantly higher in SIM2*i* cells (Fig. 5D). Cotransfection of the MMP2 reporter and increasing amounts of SIM2s expression vector in MCF-7 cells resulted in dose-dependent inhibition of luciferase activity (Fig. 5E). While we did not see the expected increase in MMP3 secretion in SIM2*i* MCF-7 cells (20), we hypothesize that this may be due to intrinsic differences between MDA-MB-435 and MCF-7 cells. Breast cancer cell lines and primary breast tumors often have dramatically different molecular signatures. Therefore, differences in MMP regulation between the cell types following modulation of SIM2s expression are probably due to inherent, as yet uncharacterized, molecular processes.

**SIM2s participates in the maintenance of E-cadherin expression via repression of Slug.** The loss of E-cadherin and keratin 18 with gain of N-cadherin and vimentin expression in SIM2*i* MCF-7 cells suggests that SIM2s may regulate factors involved in EMT. Members of the SNAIL family of transcription factors have been implicated in regulation of both normal and pathological EMT events (8, 27, 28, 41). During cancer

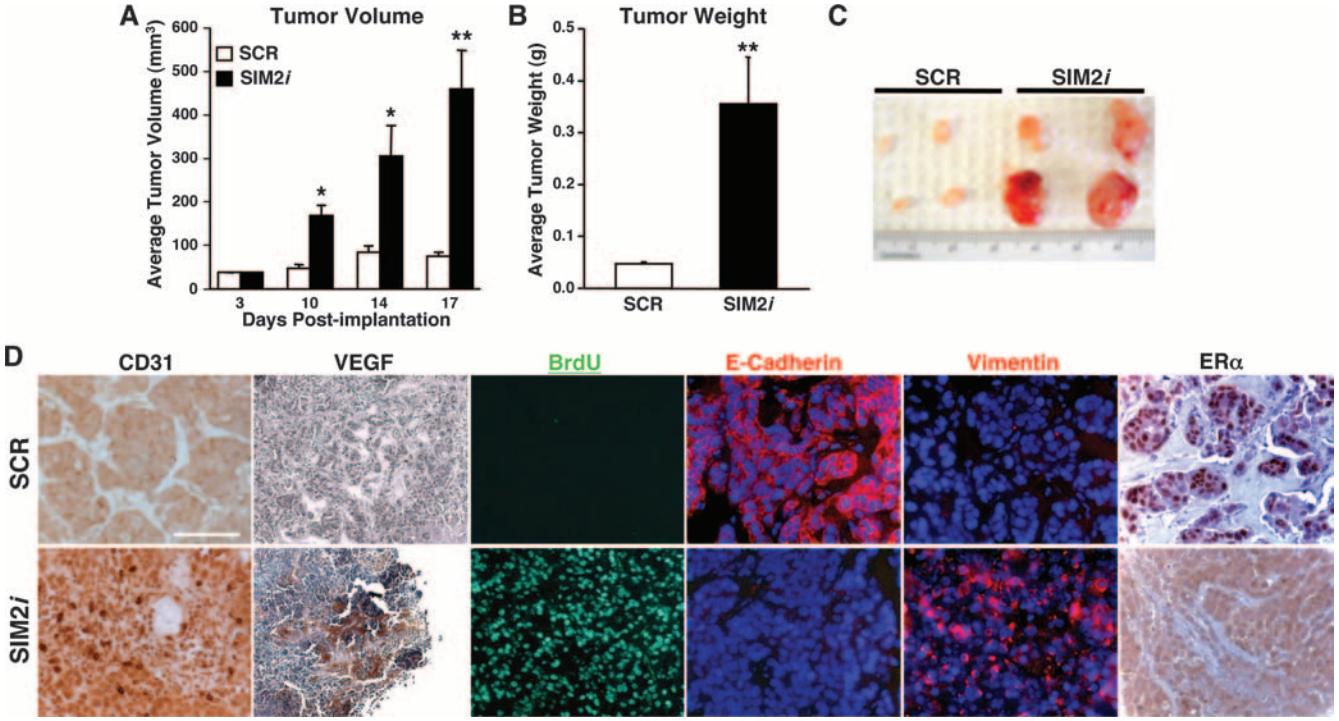


FIG. 3. Loss of SIM2s enhances in vivo tumorigenicity. Control (SCR) and SIM2*i* MCF-7 cells were mixed with growth factor-reduced Matrigel and injected into the flanks of nude mice to determine the effects of SIM2s loss on tumor growth. The mice were palpated, and tumors were measured over a period of 17 days. On the day of harvest, the mice were injected with BrdU and sacrificed 2 hours later. The tumors were removed, weighed, photographed, and fixed in 4% paraformaldehyde for subsequent analyses. (A) SIM2*i* MCF-7 cells rapidly formed tumors that were significantly larger than control tumors by 10 days postinjection. This trend continued throughout the study. The data are represented as means plus SEM; * indicates that $P$ was $<0.05$; ** indicates that $P$ was $<0.005$. (B) After 17 days, the tumors were removed and weighed. The average weight of SIM2*i*-derived tumors was significantly higher than that of control tumors. The data are represented as means plus SEM; ** indicates that $P$ was $<0.005$. (C) Representative tumors from SCR and SIM2*i* MCF-7 cells injected into nude-mouse flanks. Note the apparent increased vascularization in SIM2*i*-derived tumors. (D) Sections from SCR- and SIM2i-derived tumors were analyzed for expression of various markers by immunostaining and immunofluorescence. Increased vascularization of SIM2*i*-derived tumors is supported by increased CD31 and vascular endothelial growth factor (VEGF) protein levels seen in sections of xenograft tumors. BrdU staining indicated that SIM2i tumor cells divide at a significantly higher rate than SCR control tumors. As was seen in vitro, loss of SIM2s expression coincided with loss of E-cadherin and gain of vimentin staining in SIM2*i*-derived tumors. The apparent aggressiveness of SIM2*i*-derived tumors, and their lack of an exogenous estrogen requirement, corresponded with loss of ERα expression. Bar = 100 μm.

progression, increased SNAIL and SLUG binding to E-box regulatory DNA elements causes transcriptional repression of E-cadherin, which contributes to transformation, angiogenesis, and EMT (8, 27, 28, 41). To determine if members of the SNAIL family are involved in the EMT induced by SIM2s loss, SCR and SIM2*i* cells were analyzed for SNAIL and SLUG mRNA levels by real-time RT-PCR. SNAIL mRNA levels were not significantly affected by SIM2 loss in MCF-7 cells (Fig. 6A). In contrast, SLUG expression was up-regulated more than 250-fold in SIM2*i* cells (Fig. 6A), which corresponded to an increase in SLUG protein levels as determined by Western analysis (Fig. 6B).

Since SIM2s functions as a transcriptional repressor (18, 20, 25), we hypothesized that SIM2s directly inhibits SLUG expression at the promoter level. A luciferase reporter under the control of the human SLUG promoter was transfected into SCR and SIM2*i* MCF7 cells and analyzed for activity. In SIM2*i* MCF-7 cells, basal reporter expression was increased 10-fold over control cells (Fig. 6C). In addition, we observed concentration-dependent repression of SLUG promoter-controlled gene expression with increasing amounts of SIM2s in MCF-7 cells (Fig. 6D). The human SLUG promoter contains multiple putative regulatory elements, including E-boxes, xenobiotic response elements (XREs), and central midline element (CME) core sequences (Fig. 6E). Using an antibody to SIM2s in ChIP analyses, we found that SIM2s binds a region of the SLUG promoter containing the CME and two XRE core sequences in SCR, but not SIM2*i*, MCF-7 cells (Fig. 6E). SIM2s was unable to bind a region of the E-cadherin promoter containing E-boxes that were targeted by SNAIL protein family members; however, increased binding of SLUG to this region was apparent in SIM2*i* MCF-7 cells (Fig. 6F). As the ChIP primers used in our study flank the putative CME and two XREs, it seems likely that SIM2s-mediated repression of SLUG involves binding of SIM2s to one or more of these elements. Taken together, these data suggest that loss of SIM2s leads to derepression of SLUG expression and increased SLUG binding to the E-cadherin promoter, where it potentially plays a role in repressing E-cadherin transcription.

**Sim2$^{-/-}$ mammary glands display hallmarks of EMT.** Our initial analyses of Sim2$^{-/-}$ mammary outgrowths, coupled with in vitro MCF-7 cell studies, strongly suggest that loss of Sim2s

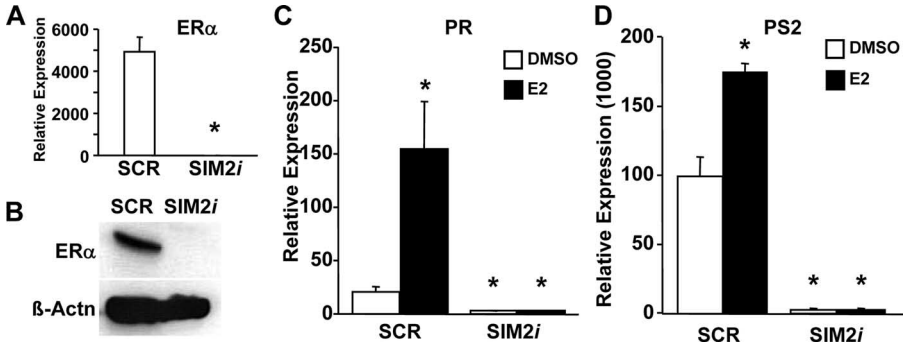


FIG. 4. Loss of ERα expression and estrogen responsiveness in SIM2*i* MCF-7 cells. (A) Quantitative real-time PCR analysis of control (SCR) and SIM2i MCF-7 cells for ERα RNA. The data were obtained from three wells per group and analyzed by the $\Delta\Delta CT$ method and are expressed as the average difference plus SEM; *, $P > 0.05$. (B) Western analysis of SCR and SIM2*i* MCF-7 cells corroborated the mRNA data and confirmed that loss of SIM2s expression results in loss of ERα. β-Actn, β-actin. (C and D) Quantitative real-time PCR analysis of vehicle (DMSO)- and estradiol (E2)-treated SCR and SIM2*i* MCF-7 cells indicated that estrogen responsiveness is lost in SIM2*i* cells. Both progesterone receptor (C) and PS2 (D) mRNA induction following estradiol treatment was lost in SIM2*i* cells. The data are presented as the average difference plus SEM; *, $P > 0.05$.

expression leads to an EMT. To confirm this in vivo, $Sim2^{-/-}$ mammary sections were analyzed for various epithelial and mesenchymal markers. Robust E-cadherin staining was observed throughout WT mammary epithelium but was totally absent in $Sim2^{-/-}$ glands (Fig. 7A). Not surprisingly, the increased invasive ability of $Sim2^{-/-}$ epithelial cells was associated with increased Mmp2 protein levels (Fig. 7A). These observations strongly suggest that an EMT similar to that observed in SIM2*i* MCF-7 cells had occurred in $Sim2^{-/-}$ glands. This was further supported by increased nuclear accumulation of β-catenin in $Sim2^{-/-}$ ductal epithelium (Fig. 7A). Consistent with our model that SIM2s-mediated repression of SLUG suppresses EMT, we found increased Slug staining in $Sim2^{-/-}$ glands (Fig. 7A). Taken together, these data show that loss of

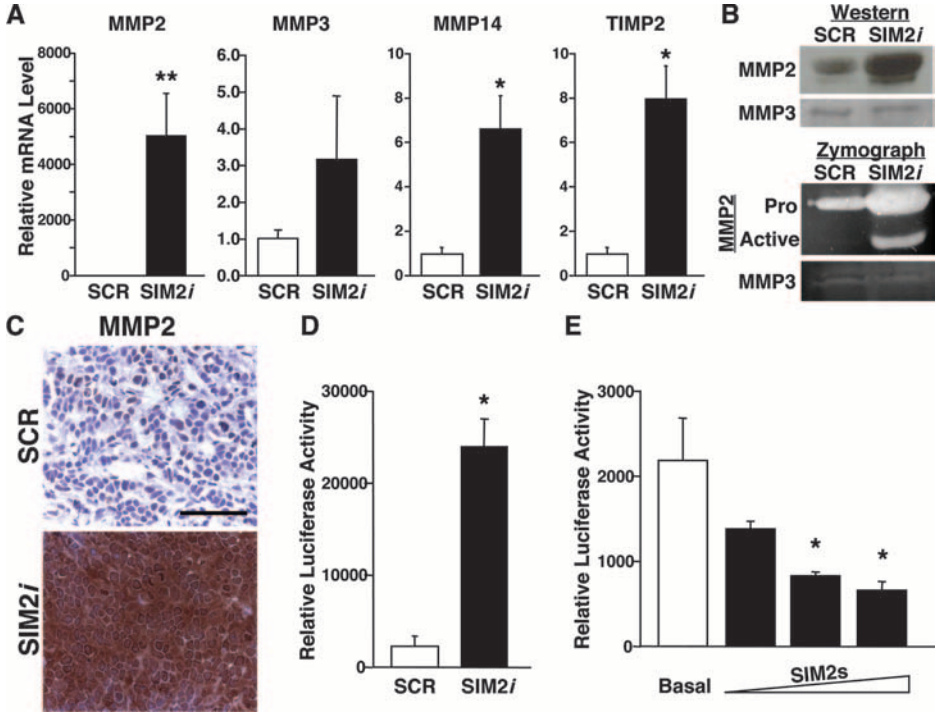


FIG. 5. SIM2s Inhibits MMP2 expression and activation. (A) Expression of MMP2, MMP14, and TIMP2, but not MMP3, was increased in SIM2*i* MCF-7 cells in comparison to control cells (SCR). (B) Increased MMP2 mRNA corresponded to increased MMP2 protein (top) and activity (bottom) in SIM2*i* MCF-7 cells with no effect on MMP3 protein or activity. (C) Immunostaining of SCR- and SIM2*i*-derived tumor sections indicated that MMP2 expression was significantly elevated in SIM2*i*-derived tumors. Bar = 100 μm. (D) Basal expression of an MMP2 promoter-controlled reporter was significantly elevated in SIM2*i* cells, suggesting that SIM2s can directly repress MMP2 expression. (E) This hypothesis is supported by the dose-dependent effects of SIM2s on repression of an MMP2-controlled reporter. The data are represented as means plus SEM; * indicates that $P$ was $<0.05$; ** indicates that $P$ was $<0.005$.

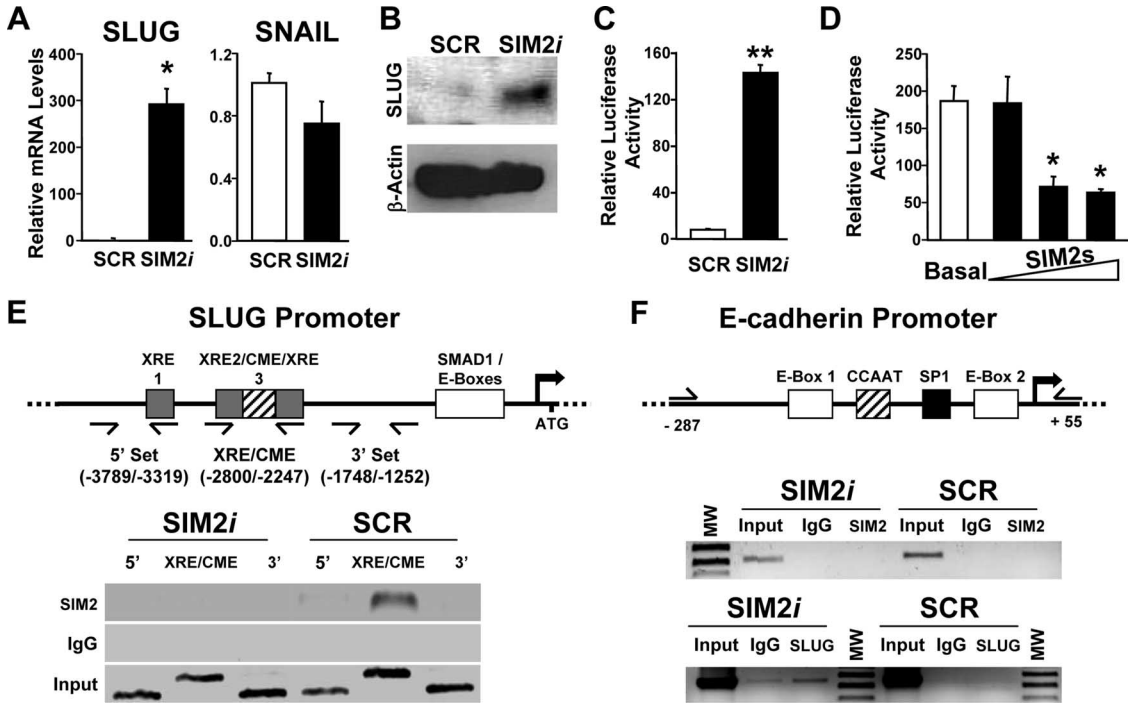


FIG. 6. SIM2s binds and represses expression from the SLUG promoter. (A) SLUG, but not SNAIL, mRNA levels were significantly reduced following loss of SIM2s expression in MCF-7 cells. (B) Increased SLUG mRNA observed in SIM2*i* cells corresponded to significantly elevated SLUG protein levels, as measured by Western blotting. (C) Expression of a SLUG promoter-controlled reporter was significantly increased in SIM2*i* MCF-7 cells. The data are represented as means plus SEM; ∗ indicates that $P$ was $<0.05$. (D) SIM2s-mediated repression of SLUG is dose dependent, as increasing amounts of SIM2s expression vector repressed expression of the SLUG reporter. The data are represented as means plus SEM; ∗∗ indicates that $P$ was $<0.005$. (E) Several putative regulatory regions are present in the first 3,280 bp of the SLUG promoter (top). ChIP analysis using an antibody to SIM2 was used to ascertain SIM2s binding to the SLUG promoter in SCR and SIM2*i* MCF-7 cells. Precipitated chromatin was assayed for the presence of SLUG promoter DNA surrounding a region containing a CME and multiple XRE consensus sequences using primers as indicated by the arrows in the promoter schematic. SIM2s protein peaked in the center of this region and was detectable in this region of the SLUG promoter in SCR control cells only. (F) SLUG and SIM2s binding to the E-cadherin promoter was analyzed in SCR and SIM2*i* MCF-7 cells by ChIP analyses. A schematic representation of the human E-cadherin promoter from −287 to +55 with respect to the transcriptional start point shows putative E-box, CCAAT enhancer binding protein, and SP1 regulatory regions, as well as the relative positions of primers used to assay for protein binding. SLUG binding to the E-cadherin promoter was detectable in SIM2*i* cells, but not in SCR cells. In contrast, SIM2s binding to the E-cadherin promoter could not be detected in either cell line.

Sim2s during mouse mammary gland ductal development results in Slug up-regulation, loss of epithelial cell characteristics, increased Mmp2 expression, and invasion of the surrounding stroma, reminiscent of an EMT (Fig. 7B).

## DISCUSSION

Based on the role of *sim* in *Drosophila* CNS development (6, 7), the developmental defects observed in Sim2$^{-/-}$ mice (12, 33), and our previous studies showing that SIM2s is expressed in human breast luminal epithelial cells and is down-regulated in breast cancers (20), we hypothesized that Sim2 contributes to normal mammary gland development. Indeed, we found that Sim2s is the primary Sim2 isoform expressed in the developing mouse mammary gland and that loss of Sim2s results in abnormal mammary-ductal morphology manifested by failure of the ducts to hollow, increased cell division, disruption of the basement membrane, and invasion of the surrounding stroma (Fig. 1). Sim2$^{-/-}$ mammary glands displayed several hallmarks of EMT, including loss of E-cadherin, nuclear accumulation of active β-catenin, and increased expression of the invasion-associated Mmp2 gene (Fig. 7). Together, these results suggest that Sim2s plays an important role in establishing and/or maintaining mammary cell fate.

Using an in vitro approach to knock down SIM2s expression in human breast cancer cells, we established that SIM2s is also a barrier to mammary cell transformation and tumor progression. The tumor-suppressive effects of SIM2s in mammary epithelial cells appeared to depend, in part, on its ability to suppress pathological EMT events initiated by SLUG (Fig. 6). We have recently demonstrated that SIM2s is decreased in human breast tumors and has tumor-suppressive activity when reintroduced into highly invasive cancer cells (20). This hypothesis is further supported by the data presented here. Down-regulation of SIM2s in MCF-7 cells resulted in loss of epithelial characteristics, increased invasion, and in vivo tumorigenesis. Furthermore, tumors arising from SIM2*i* MCF-7 cells developed rapidly and were ERα$^{-}$ and highly vascularized (Fig. 3). Our present studies have also shed light on the mechanistic basis of the tumor-suppressive properties of SIM2s. We have demonstrated that SIM2s directly represses transactivation of the SLUG and MMP promoters, which corresponds to elevated Slug and Mmp2 gene expression in Sim2$^{-/-}$ mammary epithelium (Fig. 6 and 7). To our knowl-

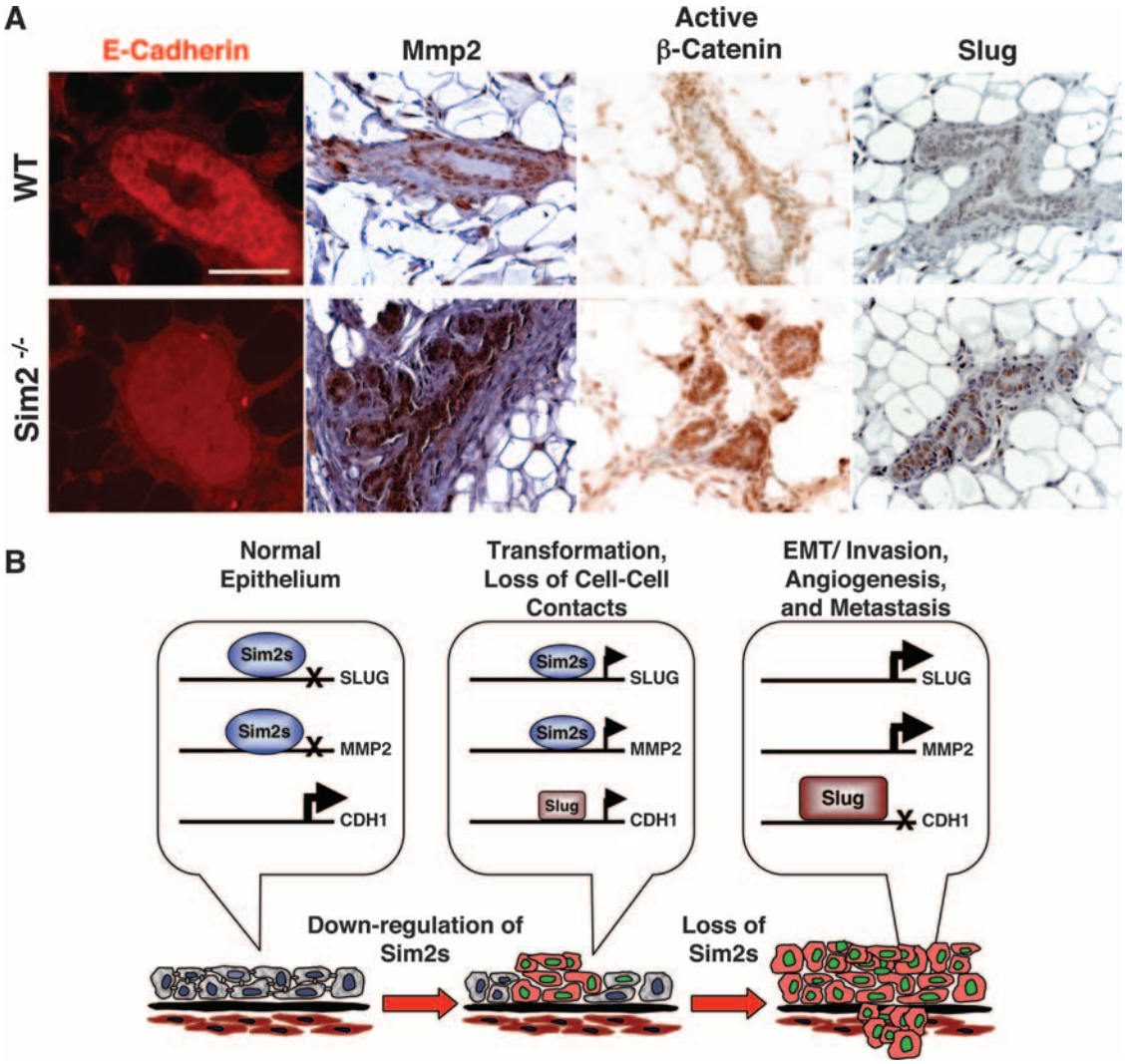


FIG. 7. Loss of Sim2s in the mouse mammary gland results in a phenotype consistent with EMT. (A) Analysis of mouse mammary outgrowths from WT and Sim2$^{-/-}$ mice revealed that loss of Sim2s expression is associated with EMT events, including loss of E-cadherin, up-regulation of Mmp2, and increased activation of β-catenin. Consistent with our hypothesis that Sim2s-mediated down-regulation of Slug represses EMT, we found that Slug protein levels were significantly elevated in Sim2$^{-/-}$ mammary glands. (B) Proposed model of Sim2 effects on mammary gland ductal development and cancer. During normal mammary gland development, Sim2s is expressed in differentiated mammary epithelial cells lining the ducts and alveoli, where it represses Slug, Mmp2, and possibly other factors promoting EMT and motility. During early transformation, Sim2s expression is decreased, allowing Slug and Mmp2 expression to increase, leading to disruption of cell-to-cell contacts and degradation of the surrounding extracellular matrix. As tumorigenesis progresses, Sim2s expression is lost and cancer cells become highly motile and aggressively invade the surrounding stroma as metastasis is initiated.

edge, these results make SIM2s the first known transcriptional repressor of SLUG and suggest that SIM2s regulation of these genes may be important for its tumor suppressor function in vivo. We propose a model in which progressive loss of SIM2s results in derepression of Slug and Mmp2, promoting E-cadherin loss, increased mitosis, angiogenesis, cell motility, and invasiveness (Fig. 7B).

The morphological and biochemical changes observed in SIM2 shRNA MCF-7 cells and Sim2$^{-/-}$ mammary glands may be interpreted as an EMT. However, there is fierce debate about the relevance of EMT to human cancers, as EMT is rarely observed in human tumor biopsies (19, 21, 39, 40). While SIM2*i* cells ceased expressing epithelial markers and Sim2$^{-/-}$ mammary epithelium displayed signs of EMT, neither acquired the mesenchymal markers fibronectin and smooth muscle actin (data not shown). Additionally, SIM2*i* MCF-7 cells retained cell junctions that appeared to contain N- instead of E-cadherin, and neither N-cadherin nor vimentin expression was observed in Sim2$^{-/-}$ mammary glands, which also appeared to have intact cell-cell junctions (not shown). A possible explanation is that loss of SIM2s does indeed induce EMT but that pathological EMTs are more heterogeneous in manifestation than an EMT occurring during normal developmental processes. Another possibility is that SIM2*i* MCF-7 and Sim2$^{-/-}$ mammary epithelial cells are examples of the recently proposed "metastable" phenotype (21). Savagner and others have described the metastable phenotype as a fusion of epithelial and mesenchymal characteristics within a single cancer

cell. Since SIM2s suppresses invasion-associated proteins (MMPs) in addition to SLUG, it may be that loss of SIM2s makes full EMT unnecessary for achieving optimal malignancy. This is apparent when we compare SIM2*i* MCF-7 cells grown in culture to those placed in the flanks of nude mice. In culture, SIM2*i* MCF-7 cells displayed a mesenchymal morphology not observed in SIM2*i* MCF-7 tumors. Similarly, the degrees of E-cadherin loss and N-cadherin and vimentin upregulation in SIM2*i* MCF-7 cells were much greater in culture than in nude mice. Such observations are consistent with the hypothesized epithelial-mesenchymal plasticity of metastable cells and may explain how cells can rapidly metastasize without displaying characteristics of a full-blown EMT. It is possible that sufficient time had not passed to complete the full EMT program in both SIM2*i* MCF-7 and $Sim2^{-/-}$ mammary epithelial cells. However, in light of how quickly SIM2*i* MCF-7 cells formed tumors, it is unlikely that complete EMT is necessary to achieve the pathogenic effects of SIM2s loss. Indeed, our data suggest that progressive reductions in SIM2s expression may transform epithelial cells and advance them rapidly through progression to malignancy. While other studies have implicated SIM2s as a tumor promoter (1, 9, 13), our present and previous studies (20) point to a tumor suppressor role for SIM2s. This suggests either that SIM2s has profoundly different tissue-specific functions or that SIM2s can have both tumor-suppressive and tumor-promoting effects depending upon the cellular context. A similar mechanism has been shown to govern the effects of transforming growth factor β in breast cancer cells, which require a specific balance of CCAAT/enhancer binding protein β isoforms to inhibit the cell cycle (11).

These studies provide compelling new evidence that SIM2s is required for proper mammary gland development and that it is a mammary tumor suppressor gene. SIM2s appears to do this, in part, by directly binding the SLUG promoter to repress its expression (Fig. 6). In addition to regulating EMT, recent evidence has shown that SLUG gene expression is associated with basal-like breast carcinoma and is required for in vitro expansion of ductal breast cancer stem/progenitor cells (35). If so, it will be interesting to determine if SIM2s plays a role in stem cell maintenance. Intriguingly, SLUG has also been implicated in palate formation (25), and $Sim2^{-/-}$ mice have palate abnormalities (29, 33), suggesting a connection between SIM2 and SLUG in regulating palatogenesis, a process requiring EMT. Potential associations between SIM2 and SLUG in palatogenesis are also supported by the observation that facial clefting is elevated in Down syndrome patients, who might be expected to have higher levels of SIM2 due to trisomy 21 (18). Intuitively, if SIM2s is a tumor suppressor, overexpression would be antitumorigenic. This is supported by the observation that individuals with Down syndrome are less susceptible to solid tumors (2, 14–16, 31, 32) and that Down syndrome provides the highest known protection against breast cancer (2). In light of our observations that SIM2s expression is lost in human breast cancers (20) and that loss of SIM2s promotes EMT and tumorigenesis in human breast cancer cells, it is tempting to speculate that increased expression of SIM2 is the root of the increased incidence of palate defects and decreased risk for solid tumors observed in Down syndrome patients (2, 14–16, 31, 32).

## ACKNOWLEDGMENTS

We thank Jeffery M. Rosen (Baylor College of Medicine, Houston, TX) for advice and critical reading of the manuscript and Michael Schamblott (Johns Hopkins University, Baltimore, MD) for providing the Sim2 knockout mice.

This study was supported by grants RO1CA111551 (W.W.P.) and RO1CA85944 (P.S.) from the National Cancer Institute, National Institutes of Environmental Health Center Award Pilot Project P30ES09106 (W.W.P.), and a Howard Hughes Predoctoral Fellowship (T.G.).

## REFERENCES

1. **Aleman, M. J., M. P. DeYoung, M. Tress, P. Keating, G. W. Perry, and R. Narayanan.** 2005. Inhibition of Single Minded 2 gene expression mediates tumor-selective apoptosis and differentiation in human colon cancer cells. Proc. Natl. Acad. Sci. USA **102:**12765–12770.
2. **Benard, J., N. Beron-Gaillard, and D. Satge.** 2005. Down's syndrome protects against breast cancer: is a constitutional cell microenvironment the key? Int. J. Cancer **113:**168–170.
3. **Blavier, L., A. Lazaryev, J. Groffen, N. Heisterkamp, Y. A. DeClerck, and V. Kaartinen.** 2001. TGF-β3-induced palatogenesis requires matrix metalloproteinases. Mol. Biol. Cell **12:**1457–1466.
4. **Chrast, R., H. S. Scott, R. Madani, L. Huber, D. P. Wolfer, M. Prinz, A. Aguzzi, H. P. Lipp, and S. E. Antonarakis.** 2000. Mice trisomic for a bacterial artificial chromosome with the single-minded 2 gene (Sim2) show phenotypes similar to some of those present in the partial trisomy 16 mouse models of Down syndrome. Hum. Mol. Genet. **9:**1853–1864.
5. **Chuang, P. T., and A. P. McMahon.** 2003. Branching morphogenesis of the lung: new molecular insights into an old problem. Trends Cell Biol. **13:**86–91.
6. **Crews, S., R. Franks, S. Hu, B. Matthews, and J. Nambu.** 1992. *Drosophila* single-minded gene and the molecular genetics of CNS midline development. J. Exp. Zool. **261:**234–244.
7. **Crews, S. T., and C. M. Fan.** 1999. Remembrance of things PAS: regulation of development by bHLH-PAS proteins. Curr. Opin. Genet. Dev. **9:**580–587.
8. **De Craene, B., F. van Roy, and G. Berx.** 2005. Unraveling signalling cascades for the Snail family of transcription factors. Cell Signal **17:**535–547.
9. **DeYoung, M. P., M. Tress, and R. Narayanan.** 2003. Down's syndrome-associated Single Minded 2 gene as a pancreatic cancer drug therapy target. Cancer Lett. **200:**25–31.
10. **Ema, M., M. Suzuki, M. Morita, K. Hirose, K. Sogawa, Y. Matsuda, O. Gotoh, Y. Saijoh, H. Fujii, H. Hamada, and Y. Fujii-Kuriyama.** 1996. cDNA cloning of a murine homologue of *Drosophila* single-minded, its mRNA expression in mouse development, and chromosome localization. Biochem. Biophys. Res. Commun. **218:**588–594.
11. **Gomis, R. R., C. Alarcon, C. Nadal, C. Van Poznak, and J. Massague.** 2006. C/EBPβ at the core of the TGFβ cytostatic response and its evasion in metastatic breast cancer cells. Cancer Cell **10:**203–214.
12. **Goshu, E., H. Jin, R. Fasnacht, M. Sepenski, J. L. Michaud, and C. M. Fan.** 2002. Sim2 mutants have developmental defects not overlapping with those of Sim1 mutants. Mol. Cell. Biol. **22:**4147–4157.
13. **Halvorsen, O. J., K. Rostad, A. M. Oyan, H. Puntervoll, T. H. Bo, L. Stordrange, S. Olsen, S. A. Haukaas, L. Hood, I. Jonassen, K. H. Kalland, and L. A. Akslen.** 2007. Increased expression of SIM2-s protein is a novel marker of aggressive prostate cancer. Clin. Cancer Res. **13:**892–897.
14. **Hasle, H., I. H. Clemmensen, and M. Mikkelsen.** 2000. Occurrence of cancer in individuals with Down syndrome. Ugeskr. Laeger. **162:**4535–4539.
15. **Hasle, H., I. H. Clemmensen, and M. Mikkelsen.** 2000. Risks of leukaemia and solid tumours in individuals with Down's syndrome. Lancet **355:**165–169.
16. **Hill, D. A., G. Gridley, S. Cnattingius, L. Mellemkjaer, M. Linet, H. O. Adami, J. H. Olsen, O. Nyren, and J. F. Fraumeni, Jr.** 2003. Mortality and cancer incidence among individuals with Down syndrome. Arch. Intern. Med. **163:**705–711.
17. **Huber, M. A., N. Kraut, and H. Beug.** 2005. Molecular requirements for epithelial-mesenchymal transition during tumor progression. Curr. Opin. Cell Biol. **17:**548–558.
18. **Kallen, B., P. Mastroiacovo, and E. Robert.** 1996. Major congenital malformations in Down syndrome. Am. J. Med. Genet. **65:**160–166.
19. **Korsching, E., J. Packeisen, C. Liedtke, D. Hungermann, P. Wulfing, P. J. van Diest, B. Brandt, W. Boecker, and H. Buerger.** 2005. The origin of vimentin expression in invasive breast cancer: epithelial-mesenchymal transition, myoepithelial histogenesis or histogenesis from progenitor cells with bilinear differentiation potential? J. Pathol. **206:**451–457.
20. **Kwak, H. I., T. Gustafson, R. P. Metz, B. Laffin, P. Schedin, and W. W. Porter.** 2006. Inhibition of breast cancer growth and invasion by single-minded 2s. Carcinogenesis **28:**259–266.
21. **Lee, J. M., S. Dedhar, R. Kalluri, and E. W. Thompson.** 2006. The epithelial-mesenchymal transition: new insights in signaling, development, and disease. J. Cell Biol. **172:**973–981.
22. **Metz, R. P., H. I. Kwak, T. Gustafson, B. Laffin, and W. W. Porter.** 2006.

Differential transcriptional regulation by mouse single-minded 2S. J. Biol. Chem. **281:**10839–10848.
23. **Miettinen, P. J., J. R. Chin, L. Shum, H. C. Slavkin, C. F. Shuler, R. Derynck, and Z. Werb.** 1999. Epidermal growth factor receptor function is necessary for normal craniofacial development and palate closure. Nat. Genet. **22:**69–73.
24. **Moffett, P., M. Dayo, M. Reece, M. K. McCormick, and J. Pelletier.** 1996. Characterization of msim, a murine homologue of the *Drosophila* sim transcription factor. Genomics **35:**144–155.
25. **Murray, S. A., K. F. Oram, and T. Gridley.** 2007. Multiple functions of Snail family genes during palate development in mice. Development **134:**1789–1797.
26. **Nakopoulou, L., E. Mylona, I. Papadaki, N. Kavantzas, I. Giannopoulou, S. Markaki, and A. Keramopoulos.** 2006. Study of phospho-beta-catenin subcellular distribution in invasive breast carcinomas in relation to their phenotype and the clinical outcome. Mod. Pathol. **19:**556–563.
27. **Peinado, H., F. Marin, E. Cubillo, H. J. Stark, N. Fusenig, M. A. Nieto, and A. Cano.** 2004. Snail and E47 repressors of E-cadherin induce distinct invasive and angiogenic properties in vivo. J. Cell Sci. **117:**2827–2839.
28. **Peinado, H., D. Olmeda, and A. Cano.** 2007. Snail, Zeb and bHLH factors in tumour progression: an alliance against the epithelial phenotype? Nat. Rev. Cancer **7:**415–428.
29. **Perez-Mancera, P. A., I. Gonzalez-Herrero, K. Maclean, A. M. Turner, M. Y. Yip, M. Sanchez-Martin, J. L. Garcia, C. Robledo, T. Flores, A. Gutierrez-Adan, B. Pintado, and I. Sanchez-Garcia.** 2006. SLUG (SNAI2) overexpression in embryonic development. Cytogenet. Genome Res. **114:**24–29.
30. **Probst, M. R., C. M. Fan, M. Tessier-Lavigne, and O. Hankinson.** 1997. Two murine homologs of the *Drosophila* single-minded protein that interact with the mouse aryl hydrocarbon receptor nuclear translocator protein. J. Biol. Chem. **272:**4451–4457.
31. **Satge, D., A. J. Sasco, H. Cure, B. Leduc, D. Sommelet, and M. J. Vekemans.** 1997. An excess of testicular germ cell tumors in Down's syndrome: three case reports and a review of the literature. Cancer **80:**929–935.
32. **Satge, D., A. J. Sasco, A. Geneix, and P. Malet.** 1998. Another reason to look for tumor suppressor genes on chromosome 21. Genes Chromosomes Cancer **21:**1.
33. **Shamblott, M. J., E. M. Bugg, A. M. Lawler, and J. D. Gearhart.** 2002. Craniofacial abnormalities resulting from targeted disruption of the murine Sim2 gene. Dev. Dyn. **224:**373–380.
34. **Shook, D., and R. Keller.** 2003. Mechanisms, mechanics and function of epithelial-mesenchymal transitions in early development. Mech. Dev. **120:**1351–1383.
35. **Storci, G., P. Sansone, D. Trere, S. Tavolari, M. Taffurelli, C. Ceccarelli, T. Guarnieri, P. Paterini, M. Pariali, L. Montanaro, D. Santini, P. Chieco, and M. Bonafe.** 2007. The basal-like breast carcinoma phenotype is regulated by SLUG gene expression. J. Pathol. **214:**25–37.
36. **Sun, D., K. R. McAlmon, J. A. Davies, M. Bernfield, and E. D. Hay.** 1998. Simultaneous loss of expression of syndecan-1 and E-cadherin in the embryonic palate during epithelial-mesenchymal transformation. Int. J. Dev. Biol. **42:**733–736.
37. **Sympson, C. J., M. J. Bissell, and Z. Werb.** 1995. Mammary gland tumor formation in transgenic mice overexpressing stromelysin-1. Semin. Cancer Biol. **6:**159–163.
38. **Sympson, C. J., R. S. Talhouk, C. M. Alexander, J. R. Chin, S. M. Clift, M. J. Bissell, and Z. Werb.** 1994. Targeted expression of stromelysin-1 in mammary gland provides evidence for a role of proteinases in branching morphogenesis and the requirement for an intact basement membrane for tissue-specific gene expression. J. Cell Biol. **125:**681–693.
39. **Tarin, D., E. W. Thompson, and D. F. Newgreen.** 2005. The fallacy of epithelial mesenchymal transition in neoplasia. Cancer Res. **65:**5996–6001.
40. **Thompson, E. W., D. F. Newgreen, and D. Tarin.** 2005. Carcinoma invasion and metastasis: a role for epithelial-mesenchymal transition? Cancer Res. **65:**5991–5995.
41. **Vega, S., A. V. Morales, O. H. Ocana, F. Valdes, I. Fabregat, and M. A. Nieto.** 2004. Snail blocks the cell cycle and confers resistance to cell death. Genes Dev. **18:**1131–1143.